

## ***CP* VIOLATION IN $K_L$ DECAYS**

Updated May 2010 by L. Wolfenstein (Carnegie-Mellon University), T.G. Trippe (BNL), and C.-J. Lin (BNL).

The symmetries  $C$  (particle-antiparticle interchange) and  $P$  (space inversion) hold for strong and electromagnetic interactions. After the discovery of large  $C$  and  $P$  violation in the weak interactions, it appeared that the product  $CP$  was a good symmetry. In 1964  $CP$  violation was observed in  $K^0$  decays at a level given by the parameter  $\epsilon \approx 2.3 \times 10^{-3}$ .

A unified treatment of  $CP$  violation in  $K$ ,  $D$ ,  $B$ , and  $B_s$  mesons is given in “ $CP$  Violation in Meson Decays” by D. Kirkby and Y. Nir in this *Review*. A more detailed review including a thorough discussion of the experimental techniques used to determine  $CP$  violation parameters is given in a book by K. Kleinknecht [1]. Here we give a concise summary of the formalism needed to define the parameters of  $CP$  violation in  $K_L$  decays, and a description of our fits for the best values of these parameters.

### **1. Formalism for $CP$ violation in Kaon decay:**

$CP$  violation has been observed in the semi-leptonic decays  $K_L^0 \rightarrow \pi^\mp \ell^\pm \nu$ , and in the nonleptonic decay  $K_L^0 \rightarrow 2\pi$ . The experimental numbers that have been measured are

$$A_L = \frac{\Gamma(K_L^0 \rightarrow \pi^- \ell^+ \nu) - \Gamma(K_L^0 \rightarrow \pi^+ \ell^- \nu)}{\Gamma(K_L^0 \rightarrow \pi^- \ell^+ \nu) + \Gamma(K_L^0 \rightarrow \pi^+ \ell^- \nu)} \quad (1a)$$

$$\begin{aligned} \eta_{+-} &= A(K_L^0 \rightarrow \pi^+ \pi^-)/A(K_S^0 \rightarrow \pi^+ \pi^-) \\ &= |\eta_{+-}| e^{i\phi_{+-}} \end{aligned} \quad (1b)$$

$$\begin{aligned} \eta_{00} &= A(K_L^0 \rightarrow \pi^0 \pi^0)/A(K_S^0 \rightarrow \pi^0 \pi^0) \\ &= |\eta_{00}| e^{i\phi_{00}} . \end{aligned} \quad (1c)$$

$CP$  violation can occur either in the  $K^0-\bar{K}^0$  mixing or in the decay amplitudes. Assuming  $CPT$  invariance, the mass eigenstates of the  $K^0-\bar{K}^0$  system can be written

$$|K_S\rangle = p|K^0\rangle + q|\bar{K}^0\rangle , \quad |K_L\rangle = p|K^0\rangle - q|\bar{K}^0\rangle . \quad (2)$$

If  $CP$  invariance held, we would have  $q = p$  so that  $K_S$  would be  $CP$ -even and  $K_L$   $CP$ -odd. (We define  $|\bar{K}^0\rangle$  as  $CP$   $|K^0\rangle$ ).

$CP$  violation in  $K^0-\overline{K}^0$  mixing is then given by the parameter  $\tilde{\epsilon}$  where

$$\frac{p}{q} = \frac{(1 + \tilde{\epsilon})}{(1 - \tilde{\epsilon})}. \quad (3)$$

$CP$  violation can also occur in the decay amplitudes

$$A(K^0 \rightarrow \pi\pi(I)) = A_I e^{i\delta_I}, \quad A(\overline{K}^0 \rightarrow \pi\pi(I)) = A_I^* e^{i\delta_I}, \quad (4)$$

where  $I$  is the isospin of  $\pi\pi$ ,  $\delta_I$  is the final-state phase shift, and  $A_I$  would be real if  $CP$  invariance held. The  $CP$ -violating observables are usually expressed in terms of  $\epsilon$  and  $\epsilon'$  defined by

$$\eta_{+-} = \epsilon + \epsilon', \quad \eta_{00} = \epsilon - 2\epsilon'. \quad (5a)$$

One can then show [2]

$$\epsilon = \tilde{\epsilon} + i (\text{Im } A_0 / \text{Re } A_0), \quad (5b)$$

$$\sqrt{2}\epsilon' = ie^{i(\delta_2 - \delta_0)} (\text{Re } A_2 / \text{Re } A_0) (\text{Im } A_2 / \text{Re } A_2 - \text{Im } A_0 / \text{Re } A_0), \quad (5c)$$

$$A_L = 2\text{Re } \epsilon / (1 + |\epsilon|^2) \approx 2\text{Re } \epsilon. \quad (5d)$$

In Eqs. (5a), small corrections [3] of order  $\epsilon' \times \text{Re}(A_2/A_0)$  are neglected, and Eq. (5d) assumes the  $\Delta S = \Delta Q$  rule.

The quantities  $\text{Im } A_0$ ,  $\text{Im } A_2$ , and  $\text{Im } \tilde{\epsilon}$  depend on the choice of phase convention, since one can change the phases of  $K^0$  and  $\overline{K}^0$  by a transformation of the strange quark state  $|s\rangle \rightarrow |s\rangle e^{i\alpha}$ ; of course, observables are unchanged. It is possible by a choice of phase convention to set  $\text{Im } A_0$  or  $\text{Im } A_2$  or  $\text{Im } \tilde{\epsilon}$  to zero, but none of these is zero with the usual phase conventions in the Standard Model. The choice  $\text{Im } A_0 = 0$  is called the Wu-Yang phase convention [4], in which case  $\epsilon = \tilde{\epsilon}$ . The value of  $\epsilon'$  is independent of phase convention, and a nonzero value demonstrates  $CP$  violation in the decay amplitudes, referred to as direct  $CP$  violation. The possibility that direct  $CP$  violation is essentially zero, and that  $CP$  violation occurs only in the mixing matrix, was referred to as the superweak theory [5].

By applying  $CPT$  invariance and unitarity the phase of  $\epsilon$  is given approximately by

$$\phi_\epsilon \approx \tan^{-1} \frac{2(m_{K_L} - m_{K_S})}{\Gamma_{K_S} - \Gamma_{K_L}} \approx 43.51 \pm 0.05^\circ, \quad (6a)$$

while Eq. (5c) gives the phase of  $\epsilon'$  to be

$$\phi_{\epsilon'} = \delta_2 - \delta_0 + \frac{\pi}{2} \approx 42.3 \pm 1.5^\circ , \quad (6b)$$

where the numerical value is based on an analysis of  $\pi-\pi$  scattering using chiral perturbation theory [6]. The approximation in Eq. (6a) depends on the assumption that direct  $CP$  violation is very small in all  $K^0$  decays. This is expected to be good to a few tenths of a degree, as indicated by the small value of  $\epsilon'$  and of  $\eta_{+-0}$  and  $\eta_{000}$ , the  $CP$ -violation parameters in the decays  $K_S \rightarrow \pi^+\pi^-\pi^0$  [7], and  $K_S \rightarrow \pi^0\pi^0\pi^0$  [8]. The relation in Eq. (6a) is exact in the superweak theory, so this is sometimes called the superweak-phase  $\phi_{SW}$ . An important point for the analysis is that  $\cos(\phi_{\epsilon'} - \phi_\epsilon) \simeq 1$ . The consequence is that only two real quantities need be measured, the magnitude of  $\epsilon$  and the value of  $(\epsilon'/\epsilon)$ , including its sign. The measured quantity  $|\eta_{00}/\eta_{+-}|^2$  is very close to unity so that we can write

$$|\eta_{00}/\eta_{+-}|^2 \approx 1 - 6\text{Re } (\epsilon'/\epsilon) \approx 1 - 6\epsilon'/\epsilon , \quad (7a)$$

$$\text{Re}(\epsilon'/\epsilon) \approx \frac{1}{3}(1 - |\eta_{00}/\eta_{+-}|) . \quad (7b)$$

From the experimental measurements in this edition of the *Review*, and the fits discussed in the next section, one finds

$$|\epsilon| = (2.228 \pm 0.011) \times 10^{-3} , \quad (8a)$$

$$\phi_\epsilon = (43.5 \pm 0.7)^\circ , \quad (8b)$$

$$\text{Re}(\epsilon'/\epsilon) \approx \epsilon'/\epsilon = (1.65 \pm 0.26) \times 10^{-3} , \quad (8c)$$

$$\phi_{+-} = (43.4 \pm 0.7)^\circ , \quad (8d)$$

$$\phi_{00} - \phi_{+-} = (0.2 \pm 0.4)^\circ , \quad (8e)$$

$$A_L = (3.32 \pm 0.06) \times 10^{-3} . \quad (8f)$$

Direct  $CP$  violation, as indicated by  $\epsilon'/\epsilon$ , is expected in the Standard Model. However, the numerical value cannot be reliably predicted because of theoretical uncertainties [9]. The value of  $A_L$  agrees with Eq. (5d). The values of  $\phi_{+-}$  and  $\phi_{00} - \phi_{+-}$  are used to set limits on  $CPT$  violation [see “Tests of Conservation Laws”].

## 2. Fits for $K_L^0$ CP-violation parameters:

In recent years,  $K_L^0$  CP-violation experiments have improved our knowledge of CP-violation parameters, and their consistency with the expectations of  $CPT$  invariance and unitarity. To determine the best values of the CP-violation parameters in  $K_L^0 \rightarrow \pi^+ \pi^-$  and  $\pi^0 \pi^0$  decay, we make two types of fits, one for the phases  $\phi_{+-}$  and  $\phi_{00}$  jointly with  $\Delta m$  and  $\tau_S$ , and the other for the amplitudes  $|\eta_{+-}|$  and  $|\eta_{00}|$  jointly with the  $K_L^0 \rightarrow \pi\pi$  branching fractions.

**Fits to  $\phi_{+-}$ ,  $\phi_{00}$ ,  $\Delta\phi$ ,  $\Delta m$ , and  $\tau_S$  data:** These are joint fits to the data on  $\phi_{+-}$ ,  $\phi_{00}$ , the phase difference  $\Delta\phi = \phi_{00} - \phi_{+-}$ , the  $K_L^0 - K_S^0$  mass difference  $\Delta m$ , and the  $K_S^0$  mean life  $\tau_S$ , including the effects of correlations.

Measurements of  $\phi_{+-}$  and  $\phi_{00}$  are highly correlated with  $\Delta m$  and  $\tau_S$ . Some measurements of  $\tau_S$  are correlated with  $\Delta m$ . The correlations are given in the footnotes of the  $\phi_{+-}$  and  $\phi_{00}$  sections of the  $K_L^0$  Listings, and the  $\tau_S$  section of the  $K_S^0$  Listings.

In most cases, the correlations are quoted as 100%, *i.e.*, with the value and error of  $\phi_{+-}$  or  $\phi_{00}$  given at a fixed value of  $\Delta m$  and  $\tau_S$ , with additional terms specifying the dependence of the value on  $\Delta m$  and  $\tau_S$ . These cases lead to diagonal bands in Figs. [1] and [2]. The KTeV experiment [10] quotes its results as values of  $\phi_{+-}$ ,  $\Delta m$ , and  $\tau_S$  with correlations, leading to the ellipses labeled “b.”

The data on  $\tau_S$ ,  $\Delta m$ , and  $\phi_{+-}$  shown in Figs. [1] and [2] are combined with data on  $\phi_{00}$  and  $\phi_{00} - \phi_{+-}$  in two fits, one without assuming  $CPT$ , and the other with this assumption. The results without assuming  $CPT$  are shown as ellipses labeled “a.” These ellipses are seen to be in good agreement with the superweak phase

$$\phi_{SW} = \tan^{-1} \left( \frac{2\Delta m}{\Delta\Gamma} \right) = \tan^{-1} \left( \frac{2\Delta m \tau_S \tau_L}{\hbar(\tau_L - \tau_S)} \right). \quad (9)$$

In Figs. [1] and [2],  $\phi_{SW}$  is shown as narrow bands labeled “j.”

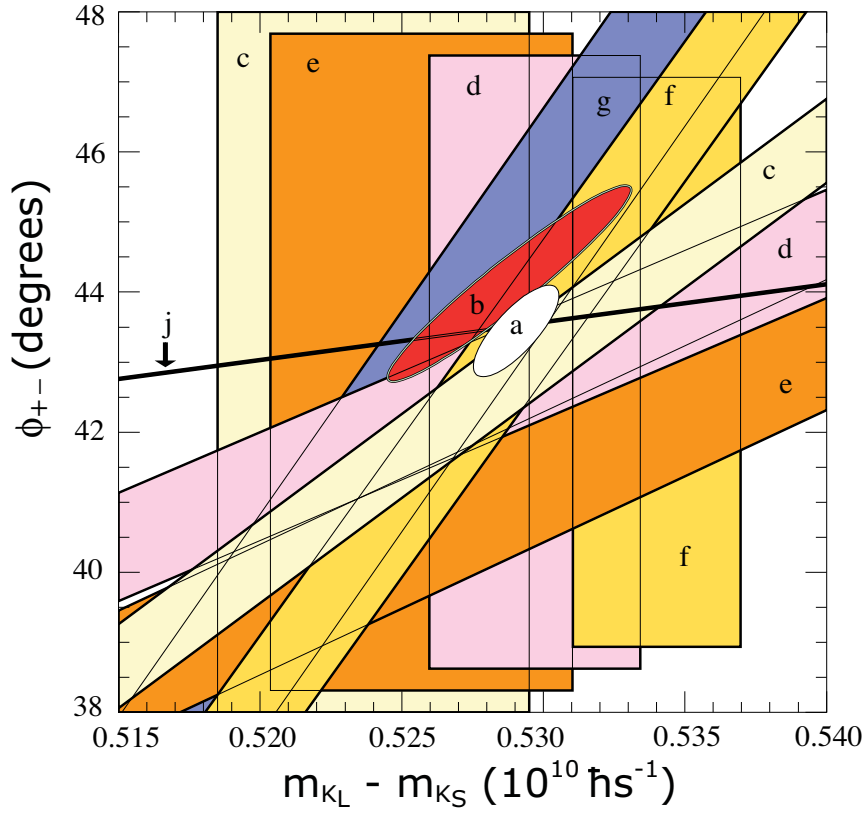


**Figure 1:**  $\phi_{+-}$  vs  $\Delta m$  for experiments which do not assume *CPT* invariance.  $\Delta m$  measurements appear as vertical bands spanning  $\Delta m \pm 1\sigma$ , cut near the top and bottom to aid the eye. Most  $\phi_{+-}$  measurements appear as diagonal bands spanning  $\phi_{+-} \pm \sigma_\phi$ . Data are labeled by letters: “b”–FNAL KTeV, “c”–CERN CPLEAR, “d”–FNAL E773, “e”–FNAL E731, “f”–CERN, “g”–CERN NA31, and are cited in Table 1. The narrow band “j” shows  $\phi_{SW}$ . The ellipse “a” shows the  $\chi^2 = 1$  contour of the fit result.

Color version at end of book.

Table 2 column 2, “Fit w/o *CPT*,” gives the resulting fitted parameters, while Table 3 gives the correlation matrix for this fit. The white ellipses labeled “a” in Fig. 1 and Fig. 2 are the  $\chi^2 = 1$  contours for this fit.

For experiments which have dependencies on unseen fit parameters, that is, parameters other than those shown on the x or y axis of the figure, their band positions are evaluated using the fit results and their band widths include the fitted

**Table 1:** References, Document ID’s, and sources corresponding to the letter labels in the figures. The data are given in the  $\phi_{+-}$  and  $\Delta m$  sections of the  $K_L$  Listings, and the  $\tau_s$  section of the  $K_S$  Listings.

Label	Source	PDG Document ID	Ref.
a	this <i>Review</i>	OUR FIT	
b	FNAL KTeV	ALAVI-HARATI 03	[10]
c	CERN CPLEAR	APOSTOLAKIS 99C	[11]
d	FNAL E773	SCHWINGENHEUER 95	[12]
e	FNAL E731	GIBBONS 93,93C	[13,14]
f	CERN	GEWENIGER 74B,74C	[15,16]
g	CERN NA31	CAROSI 90	[17]
h	CERN NA48	LAI 02C	[18]
i	CERN NA31	BERTANZA 97	[19]
j	this <i>Review</i>	SUPERWEAK 10	

uncertainty in the unseen parameters. This is also true for the  $\phi_{\text{SW}}$  bands.

If  $CPT$  invariance and unitarity are assumed, then by Eq. (6a), the phase of  $\epsilon$  is constrained to be approximately equal to

$$\phi_{\text{SW}} = (43.5165 \pm 0.0002)^\circ + 54.1(\Delta m - 0.5290)^\circ + 32.0(\tau_s - 0.8958) \quad (10)$$

where we have linearized the  $\Delta m$  and  $\tau_s$  dependence of Eq. (9). The error  $\pm 0.0002$  is due to the uncertainty in  $\tau_L$ . Here  $\Delta m$  has units  $10^{10} \hbar \text{s}^{-1}$  and  $\tau_s$  has units  $10^{-10} \text{s}$ .

If in addition we use the observation that  $\text{Re}(\epsilon'/\epsilon) \ll 1$  and  $\cos(\phi_{\epsilon'} - \phi_\epsilon) \simeq 1$ , as well as the numerical value of  $\phi_{\epsilon'}$  given in Eq. (6b), then Eqs. (5a), which are sketched in Fig. 3, lead to the constraint

$$\begin{aligned} \phi_{00} - \phi_{+-} &\approx -3 \text{ Im} \left( \frac{\epsilon'}{\epsilon} \right) \\ &\approx -3 \text{ Re} \left( \frac{\epsilon'}{\epsilon} \right) \tan(\phi_{\epsilon'} - \phi_\epsilon) \\ &\approx 0.006^\circ \pm 0.008^\circ , \end{aligned} \quad (11)$$

so that  $\phi_{+-} \approx \phi_{00} \approx \phi_\epsilon \approx \phi_{\text{SW}}$ .

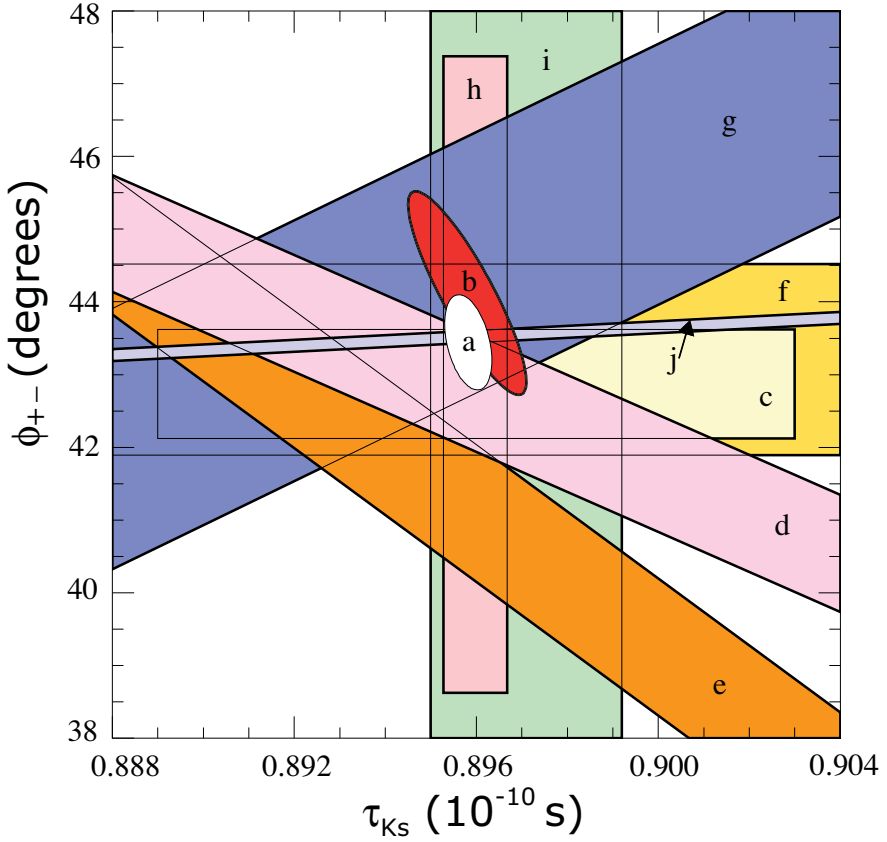


**Figure 2:**  $\phi_{+-}$  vs  $\tau_s$ .  $\tau_s$  measurements appear as vertical bands spanning  $\tau_s \pm 1\sigma$ , some of which are cut near the top and bottom to aid the eye. Most  $\phi_{+-}$  measurements appear as diagonal or horizontal bands spanning  $\phi_{+-} \pm \sigma_\phi$ . Data are labeled by letters: “b”–FNAL KTeV, “c”–CERN CPLEAR, “d”–FNAL E773, “e”–FNAL E731, “f”–CERN, “g”–CERN NA31, “h”–CERN NA48, “i”–CERN NA31, and are cited in Table 1. The narrow band “j” shows  $\phi_{\text{SW}}$ . The ellipse “a” shows the fit result’s  $\chi^2 = 1$  contour. Color version at end of book.

In the fit assuming *CPT*, we constrain  $\phi_\epsilon = \phi_{\text{SW}}$  using the linear expression in Eq. (10), and constrain  $\phi_{00} - \phi_{+-}$  using Eq. (11). These constraints are inserted into the Listings with the Document ID of SUPERWEAK 10. Some additional data for which the authors assumed *CPT* are added to this fit or substitute for other less precise data for which the authors did not make this assumption. See the Listings for details.

**Table 2:** Fit results for  $\phi_{+-}$ ,  $\Delta m$ ,  $\tau_s$ ,  $\phi_{00}$ ,  $\Delta\phi = \phi_{00} - \phi_{+-}$ , and  $\phi_\epsilon$  without and with the *CPT* assumption.

Quantity(units)	Fit w/o <i>CPT</i>	Fit w/ <i>CPT</i>
$\phi_{+-}(\circ)$	$43.4 \pm 0.7$ (S=1.3)	$43.51 \pm 0.05$ (S=1.1)
$\Delta m(10^{10}\hbar s^{-1})$	$0.5290 \pm 0.0015$ (S=1.1)	$0.5292 \pm 0.0009$ (S=1.2)
$\tau_s(10^{-10}s)$	$0.8958 \pm 0.0005$	$0.8953 \pm 0.0005$ (S=1.1)
$\phi_{00}(\circ)$	$43.7 \pm 0.8$ (S=1.2)	$43.52 \pm 0.05$ (S=1.1)
$\Delta\phi(\circ)$	$0.2 \pm 0.4$	$0.006 \pm 0.014$ (S=1.8)
$\phi_\epsilon(\circ)$	$43.5 \pm 0.7$ (S=1.3)	$43.51 \pm 0.05$ (S=1.1)
$\chi^2$	17.4	21.9
# Deg. Free.	13	17

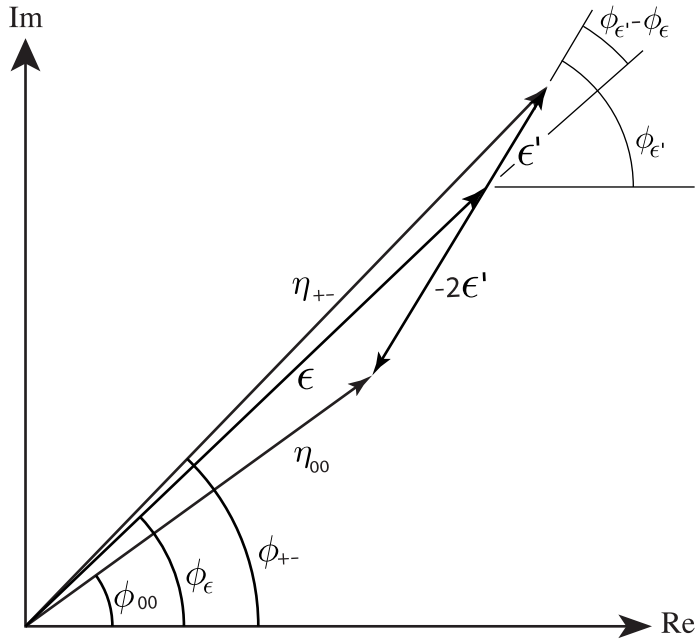


**Figure 3:** Sketch of Eqs. (5a). Not to scale.

The results of this fit are shown in Table 2, column 3, “Fit w/*CPT*,” and the correlation matrix is shown in Table 4. The  $\Delta m$  precision is improved by the *CPT* assumption.

**Table 3:** Correlation matrix for the results of the fit without the *CPT* assumption

	$\phi_{+-}$	$\Delta m$	$\tau_s$	$\phi_{00}$	$\Delta\phi$	$\phi_\epsilon$
$\phi_{+-}$	1.000	0.778	-0.391	0.837	-0.002	0.977
$\Delta m$	0.778	1.000	-0.424	0.665	0.024	0.766
$\tau_s$	-0.391	-0.424	1.000	-0.327	0.001	-0.382
$\phi_{00}$	0.837	0.665	-0.327	1.000	0.546	0.934
$\Delta\phi$	-0.002	0.024	0.001	0.546	1.000	0.211
$\phi_\epsilon$	0.977	0.766	-0.382	0.934	0.211	1.000

**Table 4:** Correlation matrix for the results of the fit with the *CPT* assumption

	$\phi_{+-}$	$\Delta m$	$\tau_s$	$\phi_{00}$	$\Delta\phi$	$\phi_\epsilon$
$\phi_{+-}$	1.000	0.924	0.054	0.711	-0.283	0.964
$\Delta m$	0.924	1.000	-0.231	0.834	-0.020	0.958
$\tau_s$	0.054	-0.231	1.000	0.056	0.009	0.059
$\phi_{00}$	0.711	0.834	0.056	1.000	0.473	0.873
$\Delta\phi$	-0.283	-0.020	0.009	0.473	1.000	-0.018
$\phi_\epsilon$	0.964	0.958	0.059	0.873	-0.018	1.000

### Fits for $\epsilon'/\epsilon$ , $|\eta_{+-}|$ , $|\eta_{00}|$ , and $B(K_L \rightarrow \pi\pi)$

We list measurements of  $|\eta_{+-}|$ ,  $|\eta_{00}|$ ,  $|\eta_{00}/\eta_{+-}|$ , and  $\epsilon'/\epsilon$ . Independent information on  $|\eta_{+-}|$  and  $|\eta_{00}|$  can be obtained from measurements of the  $K_L^0$  and  $K_S^0$  lifetimes ( $\tau_L$ ,  $\tau_s$ ), and branching ratios (B) to  $\pi\pi$ , using the relations

$$|\eta_{+-}| = \left[ \frac{B(K_L^0 \rightarrow \pi^+ \pi^-)}{\tau_L} \frac{\tau_s}{B(K_S^0 \rightarrow \pi^+ \pi^-)} \right]^{1/2}, \quad (12a)$$

$$|\eta_{00}| = \left[ \frac{B(K_L^0 \rightarrow \pi^0 \pi^0)}{\tau_L} \frac{\tau_s}{B(K_S^0 \rightarrow \pi^0 \pi^0)} \right]^{1/2}. \quad (12b)$$

For historical reasons, the branching ratio fits and the *CP*-violation fits are done separately, but we want to include the influence of  $|\eta_{+-}|$ ,  $|\eta_{00}|$ ,  $|\eta_{00}/\eta_{+-}|$ , and  $\epsilon'/\epsilon$  measurements on  $B(K_L^0 \rightarrow \pi^+ \pi^-)$  and  $B(K_L^0 \rightarrow \pi^0 \pi^0)$  and vice versa. We

approximate a global fit to all of these measurements by first performing two independent fits: 1) BRFIT, a fit to the  $K_L^0$  branching ratios, rates, and mean life, and 2) ETAFIT, a fit to the  $|\eta_{+-}|$ ,  $|\eta_{00}|$ ,  $|\eta_{+-}/\eta_{00}|$ , and  $\epsilon'/\epsilon$  measurements. The results from fit 1, along with the  $K_S^0$  values from this edition, are used to compute values of  $|\eta_{+-}|$  and  $|\eta_{00}|$ , which are included as measurements in the  $|\eta_{00}|$  and  $|\eta_{+-}|$  sections with a document ID of BRFIT 10. Thus, the fit values of  $|\eta_{+-}|$  and  $|\eta_{00}|$  given in this edition include both the direct measurements and the results from the branching ratio fit.

The process is reversed in order to include the direct  $|\eta|$  measurements in the branching ratio fit. The results from fit 2 above (before including BRFIT 10 values) are used along with the  $K_L^0$  and  $K_S^0$  mean lives and the  $K_S^0 \rightarrow \pi\pi$  branching fractions to compute the  $K_L^0$  branching ratio  $\Gamma(K_L^0 \rightarrow \pi^0\pi^0)/\Gamma(K_L^0 \rightarrow \pi^+\pi^-)$ . This branching ratio value is included as a measurement in the branching ratio section with a document ID of ETAFIT 10. Thus, the  $K_L^0$  branching ratio fit values in this edition include the results of the direct measurement of  $|\eta_{00}/\eta_{+-}|$  and  $\epsilon'/\epsilon$ . Most individual measurements of  $|\eta_{+-}|$  and  $|\eta_{00}|$  enter our fits directly via the corresponding measurements of  $\Gamma(K_L^0 \rightarrow \pi^+\pi^-)/\Gamma(\text{total})$  and  $\Gamma(K_L^0 \rightarrow \pi^0\pi^0)/\Gamma(\text{total})$ , and those that do not have too large errors to have any influence on the fitted values of these branching ratios. A more detailed discussion of these fits is given in the 1990 edition of this *Review* [20].

## References

1. K. Kleinknecht, “Uncovering  $CP$  violation: experimental clarification in the neutral  $K$  meson and  $B$  meson systems,” *Springer Tracts in Modern Physics*, vol. 195 (Springer Verlag 2003).
2. B. Winstein and L. Wolfenstein, Rev. Mod. Phys. **65**, 1113 (1993).
3. M.S. Sozzi, Eur. Phys. J. **C36**, 37 (2004).
4. T.T. Wu and C.N. Yang, Phys. Rev. Lett. **13**, 380 (1964).
5. L. Wolfenstein, Phys. Rev. Lett. **13**, 562 (1964);  
L. Wolfenstein, Comm. Nucl. Part. Phys. **21**, 275 (1994).

6. G. Colangelo, J. Gasser, and H. Leutwyler, Nucl. Phys. **B603**, 125 (2001).
7. R. Adler *et al.*, (CPLEAR Collaboration), Phys. Lett. **B407**, 193 (1997);  
P. Bloch, *Proceedings of Workshop on K Physics* (Orsay 1996), ed. L. Iconomidou-Fayard, Edition Frontieres, Gif-sur-Yvette, France (1997) p. 307.
8. A. Lai *et al.*, Phys. Lett. **B610**, 165 (2005).
9. G. Buchalla, A.J. Buras, and M.E. Lautenbacher, Rev. Mod. Phys. **68**, 1125 (1996);  
S. Bosch *et al.*, Nucl. Phys. **B565**, 3 (2000);  
S. Bertolini, M. Fabrichesi, and J.O. Egg, Rev. Mod. Phys. **72**, 65 (2000).
10. A. Alavi-Harati *et al.*, Phys. Rev. **D67**, 012005 (2003);  
See also *erratum*, Alavi-Harati *et al.*, Phys. Rev. **D**, to be published, for corrections to correlation coefficients.
11. A. Apostolakis *et al.*, Phys. Lett. **B458**, 545 (1999).
12. B. Schwingenheuer *et al.*, Phys. Rev. Lett. **74**, 4376 (1995).
13. L.K. Gibbons *et al.*, Phys. Rev. Lett. **70**, 1199 (1993) and footnote in Ref. 12.
14. L.K. Gibbons, Thesis, RX-1487, Univ. of Chicago, 1993.
15. C. Geweniger *et al.*, Phys. Lett. **48B**, 487 (1974).
16. C. Geweniger *et al.*, Phys. Lett. **52B**, 108 (1974).
17. R. Carosi *et al.*, Phys. Lett. **B237**, 303 (1990).
18. A. Lai *et al.*, Phys. Lett. **B537**, 28 (2002).
19. L. Bertanza *et al.*, Z. Phys. **C73**, 629 (1997).
20. J.J. Hernandez *et al.*, Particle Data Group, Phys. Lett. **B239**, 1 (1990).